Article

pubs.acs.org/Biomac

Strong, Resilient, and Sustainable Aliphatic Polyester Thermoplastic Elastomers

Annabelle Watts, Naruki Kurokawa,† and Marc A. Hillmyer*

Department of Chemistry, University of Minnesota, Minneapolis, Minnesota 55455-0431, United States of America

Supporting Information

ABSTRACT: Thermoplastic elastomers (TPEs) composed of ABA block polymers exhibit a wide variety of properties and are easily processable as they contain physical, rather than chemical, cross-links. Poly(γ-methyl-ε-caprolactone) (PγMCL) is an amorphous polymer with a low entanglement molar mass (M_e = 2.9 kg mol^{-1}), making it a suitable choice for tough elastomers. Incorporating PγMCL as the midblock with polylactide (PLA) end blocks (f_{LA} = 0.17) results in TPEs with high stresses and elongations at break (σ_B = 24 ± 2 MPa and ε_B = 1029 ± 20%, respectively) and low levels of hysteresis. The use of isotactic PLA as the end blocks (f_{LLA} = 0.17) increases the strength and toughness of the material (σ_B = 30 ± 4 MPa, ε_B = 988 ± 30%) due to its semicrystalline nature. This study aims to demonstrate how the outstanding properties in these sustainable materials are a result of the entanglements, glass transition temperature, segment−segment interaction parameter, and crystallinity, resulting in comparable properties to the commercially relevant styrene-based TPEs.

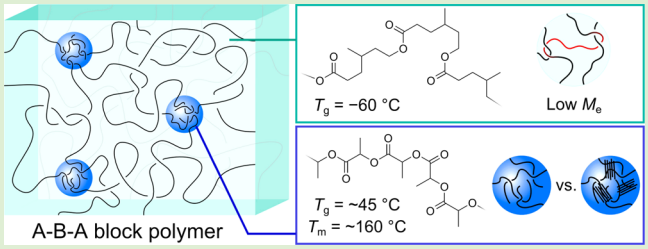

INTRODUCTION

As we experience the detrimental impacts of persistent plastics, there have been significant efforts to investigate methods to circumvent the negative consequences of our plastic society. The polymer industry relies heavily on the use of nonrenewable feedstocks and the generation of nondegradable products. Though some of these materials synthesized can be efficiently recycled or harvested for energy, some estimates suggest that 40% of the produced plastic packaging ends up in the landfill and 32% leaks into the environment.[1] Expanding the implementation of green chemistry principles for polymer research is important for the future of plastics.[2,3] By designing practical approaches that employ safe, nontoxic chemicals while limiting waste and energy, useful materials from sustainable resources can be generated and implemented.

Thermoplastic elastomers (TPEs) include ABA triblock copolymers that are typically composed of polystyrene (PS) as the glassy A block and polyisoprene (PI) or polybutadiene (PB; and hydrogenated variants) as the rubbery B block.[4] TPEs have hard (i.e., high glass transition and/or high melting temperature) A blocks in the minority fraction that microphase separate from the soft (i.e., low glass transition temperature) B block in the majority fraction, resulting in a physically cross-linked material. The hard end blocks, connected by rubbery midblocks that usually contain trapped entanglements, allow for the materials to exhibit high ultimate tensile strength (σ_B) and strain at break (ε_B). TPEs are used in a broad range of applications such as coatings, pressure sensitive adhesives, medical devices, and automotive parts; the properties can range from hard plastics to soft rubbers, depending on composition and architecture.[4] Styrenic TPEs (PS-TPEs) are petroleum derived and are extensively used due to their versatile properties and low cost. PS-*block*-PB-*block*-PS (SBS) has comparable properties to vulcanized (i.e., chemically cross-linked) natural rubber and exceed the properties of styrene−butadiene rubber (SBR); TPEs exhibit ultimate tensile strengths up to 30 MPa and 800% strain at break.[4] The entanglement molar masses, glass transition temperatures, and the thermodynamic incompatibility between the rubbery block and the PS block all contribute to the properties exhibited in the resulting TPEs.[4−6]

Significant research efforts have utilized aliphatic polyesters, which provide inherent hydrolytic degradability to the material, as alternatives to styrenic TPEs.[7−12] Polylactide (PLA) has long been studied as a sustainable substitute for PS, and this has been extended to the utilization of PLA as the hard end blocks in TPEs. Performance of PLA-TPEs reported in literature depends on the tacticity of the PLA block and the identity of the rubbery midblock. Noncrystalline aliphatic polyester midblocks in PLA-containing TPEs reported in the literature include: poly(β-methyl-δ-valerolactone) (PβMVL),[13] poly(ε-caprolactone-*co*-δ-valerolactone),[14] poly(1,5-dioxepan-2-one),[15] poly(menthide) (PM),[16−18] poly(ε-methyl-ε-caprolactone) (PεMCL),[19] poly(ε-decalactone) (PDL),[20] and poly(ε-caprolactone-*co*-ε-decalactone) (PCD).[21] Other aliphatic polyesters such as poly(ε-caprolactone) (PCL), which is semicrystalline, and poly(ε-caprolactone-*co*-LLA), which can be amorphous or semicrystalline, have also been studied in PLA-TPEs.[22−25]

Received: February 24, 2017
Revised: April 17, 2017
Published: May 3, 2017

DOI: 10.1021/acs.biomac.7b00283
Biomacromolecules 2017, 18, 1845−1854

These aliphatic polyester systems exhibit promising mechanical properties that rival PS-based TPEs. In fact, some of these low glass transition temperature (T_g) midblocks were generated from renewable resources and thus are even more attractive from a sustainability standpoint.

PβMVL-based TPEs are among the highest performing aliphatic polyester examples, exceeding the mechanical properties of SBS in some cases.[13] From sustainable and economic standpoints, PβMVL is an attractive target as the soft segment in TPEs. However, the low ceiling temperature for the polymerization of βMVL can lead to significant levels of residual monomer present at equilibrium when using reaction conditions at or above room temperature for neat monomer.[26] This in turn necessitates the rigorous removal of catalyst or some postmodification to limit complications from depolymerization.[27] The polymerization of ε-caprolactone derivatives are more thermodynamically driven toward the formation of polymer and do not face the same issues of high equilibrium monomer concentration at typical melt polymerization temperatures.[28,29] For example, the melt polymerization of ε-caprolactone at 130 °C reaches an equilibrium conversion of ~99%, whereas the same polymerization of the constitutional isomer βMVL reaches an equilibrium conversion of 57%.[13,30]

Though polymerizations of substituted ε-caprolactones are thermodynamically favorable, the position of the substituents in the ε-position impacts the rates of polymerization. The position of the methyl substituent at the γ-position exhibits faster rates of polymerization than the substituent at the ε-position, in both enzymatic and metal-catalyzed polymerizations.[31] Moreover, the polymerization of γ-methyl-ε-caprolactone (γMCL) is known to be faster than γ-substituted ε-caprolactones with longer alkyl chains (ethyl, butyl, and propyl substituents).[32] The low glass transition temperature of PγMCL (T_g = −61 °C) has motivated the use of this polymer in biomedical applications.[33−40] Combined, these attributes make PγMCL an interesting and desirable polymer to incorporate into PLA-TPEs. Moreover, γMCL can be synthesized through the Baeyer−Villiger oxidation of 4-methylcyclohexanone, a molecule that can ultimately be sourced from cresols. Although cresols exist in nature, the major sources of cresols are from petroleum products and coal tar.[41] Recent efforts that demonstrate the transformation of renewable feedstocks into cresols provide enticing and practical routes to sustainably sourced γMCL.[42−44] Two particularly attractive approaches that hold tremendous promise are shown in Scheme 1.

In this work, we report the use of PγMCL as the rubbery block in ABA triblock polymers with PLA as the end blocks to yield high performance PLA-TPEs. Furthermore, we utilize the system PLA-*block*-PγMCL-*block*-PLA (LA-γMCL-LA) as a platform to better understand the effect of entanglements, microphase separation, and T_g in PLA-based TPEs. We also provide evidence for how crystallinity in the PLA end block improves mechanical properties. These results are compared to the properties and trends that have been studied in PS-based TPEs.

EXPERIMENTAL SECTION

Materials. Chloroform, dichloromethane, methanol, and hexanes were obtained from Fisher Scientific and used without further purification. Lactide was generously provided by Altasorb (a subsidiary of Ortec, Inc.). All other chemicals were used as received from Sigma-Aldrich unless otherwise specified. Lactide and 1,4-benzenedimethanol were recrystallized from toluene (×3), dried under vacuum for 48 h, and stored under inert atmosphere. Sn(Oct)$_2$ was distilled three times under vacuum with argon (30−50 mTorr, 130−150 °C) before storing under an inert atmosphere. Anhydrous toluene was obtained through a JC Meyer solvent drying system.

Scheme 1. Proposed Retro-Synthetic Analysis of the Synthesis of γ-Methyl-ε-caprolactone from Renewable Feedstocks[42,43]

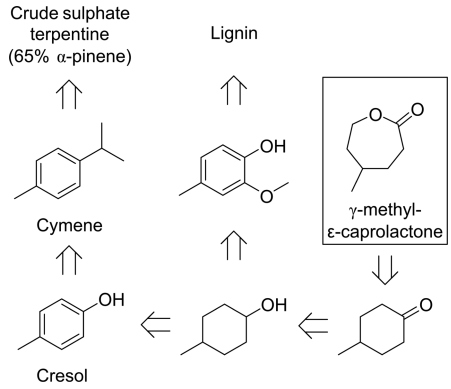

Characterization. Bruker Avance III 500 was used for ^{1}H and ^{13}C NMR spectroscopy. Molar masses were calculated from end-group analysis. Thermal properties were obtained using a TA Instruments Discovery DSC. Samples were prepared in hermetically sealed pans and heated at 10 °C min^{-1} to 200 °C to erase any thermal history, cooled to −80 °C, and data was collected from the second heat cycle (unless otherwise indicated). Size exclusion chromatography was performed on an Agilent 1100 series SEC with HP1047A refractive index detector using a chloroform mobile phase at 35 °C through 3 Varian PLgel Mixed C Columns at 1 mL min^{-1}. Relative molar mass was determined from a calibration curve created using PS standards purchased from Polymer Laboratories. Polymer density was determined by making solutions of ethylene glycol and water to obtain solutions of varying density, and a bubble-free polymer sample was dropped in the solutions to determine if it would sink or float.

Triblock copolymers were placed between two Teflon sheets and melt-pressed at 70−180 °C for 3 min then quenched to room temperature using water cooling (~35 °C min^{-1}) through the hot press.[45] Dog-bone-shaped tensile bars were punched out, resulting in samples with approximately 0.5 mm thickness, 3 mm gauge width, and 16 mm gauge length. Samples were tested to the point of break using Shimadzu Autograph AGS-X Tensile Tester and an extension rate of 50 mm min^{-1}. Using 25 mm parallel plates, TA Instruments Rheometric Series ARES instrument was used for dynamic mechanical thermal analysis (DMTA). Heating was controlled under a nitrogen atmosphere, and the samples were equilibrated at the designated temperature for 10 min before testing. To determine order−disorder temperatures, the samples were heated at 1 °C min^{-1} while applying a 1% strain and 1 rad s^{-1}. Extensional DMTA and stress relaxation analysis were performed on a TA Instruments RSA-G2 in tension mode on rectangular polymer films with 0.5 mm thickness and 3 mm gauge width. DMTA experiments were conducted at a heating rate of 5 °C min^{-1} with an oscillating strain of 0.05% and angular frequency of 1 Hz. Stress relaxation analysis was conducted after an equilibration time of 10 min at the selected temperature by applying a step strain of 25% and measuring the modulus for 3 h. Temperature control at 20 °C for LLA-γMCL-LLA was not able to be maintained over 3 h and data was not collected. SAXS experiments were conducted at the DuPont-Northwestern Dow Collaborative Access Team (DND-CAT) synchrotron research center 5-ID-D beamline of Advanced Photon Source at Argonne National Laboratory.

γ-Methyl-ε-caprolactone Synthesis. In a typical reaction, *meta*-chloroperoxybenzoic acid (110 g of 77% *m*CPBA, 490 mmol) was dissolved in methylene chloride (1.6 L, 10% w/v). After removing water that phase separated by pipet, the solution was further dried over magnesium sulfate and filtered into a round-bottom flask. The solution

DOI: 10.1021/acs.biomac.7b00283
Biomacromolecules 2017, 18, 1845−1854

was cooled to 5 °C using a salt-ice bath, and 4-methylcyclohexanone (50 g, 446 mmol) was added slowly such that the temperature was kept below 10 °C. The reaction was left to react while slowly warming up to room temperature, while *meta*-chlorobenzoic acid (*m*CBA) began to precipitate. After 4 h, the reaction was cooled in an ice bath to 5 °C and the reaction mixture was filtered to remove precipitated *m*CBA. The reaction was then concentrated to half the volume, cooled, and filtered again. The solution collected was washed carefully with freshly prepared 10% aqueous sodium bisulfite, followed by saturated sodium bicarbonate. Once neutral, the solution was dried using brine and stirred over magnesium sulfate until dry. The product was then passed through a basic alumina plug and concentrated in vacuo. The product was isolated by fractional distillation under dynamic vacuum (200−1000 mTorr, 70−100 °C). The distilled product was dried over calcium hydride overnight and then distilled, this was repeated 2−3 times (70−80% yield).

^{1}H NMR (500 MHz, chloroform-*d*) δ = 4.33−4.24 (m, 1H), 4.24−4.13 (m, 1H), 2.72−2.56 (m, 2H), 2.00−1.85 (m, 2H), 1.85−1.72 (m, 1H), 1.56−1.44 (m, 1H), 1.39−1.26 (m, 1H), 1.00 (d, J = 7.0 Hz, 3H).

Polymer Synthesis. γ-Methyl-ε-caprolactone (10 g, 78 mmol), 1,4-benzenedimethanol (43 mg, 0.31 mmol), and Sn(Oct)$_2$ (32 mg, 0.078 mmol) were added to a pressure vessel under a nitrogen atmosphere in a glovebox. (Note: pressure vessels were inspected for imperfections before use and vessels were filled below the halfway point for all reactions.) The vessel was sealed, taken out of the glovebox, and placed in a 130 °C oil bath. After 1 h, the vessel was cooled in an ice bath to stop the reaction. The clear, viscous polymer was dissolved in chloroform and precipitated into cold methanol (×1) and then hexanes (×2). A clear, viscous liquid was collected by decanting the solvent and dried by blowing nitrogen over the sample for 1 h then in vacuo for a minimum of 48 h (93−96% yield).

PγMCL ^{1}H NMR (500 MHz, chloroform-*d*) δ = 7.35 (s, 4H), 5.11 (s, 4H), 4.20−4.01 (m, 507H), 3.76−3.62 (m, 5H), 2.42−2.23 (m, 516H), 1.74−1.62 (m, 561H), 1.62−1.39 (m, 790H), 0.97−0.87 (m, 780H).

PγMCL (3 g, 0.09 mmol), lactide (3.3 g, 23 mmol), Sn(Oct)$_2$ (8 mg, 0.02 mmol), and toluene (1 mol L^{-1} monomer in solvent) were added to a pressure vessel under a nitrogen atmosphere in a glovebox. (Note: pressure vessels were inspected for imperfections before use and vessels were filled below the halfway point for all reactions.) The solution was left stirring overnight to ensure PγMCL was completely dissolved in toluene. The reaction vessel was submerged in a 130 °C oil bath for 90 min, then cooled using an ice bath. The polymer was dissolved in chloroform and precipitated into methanol (×3) and then hexanes (×1). Polymers were dried in vacuo for a minimum of 48 h (80−88% yield).

LA-γMCL-LA ^{1}H NMR (500 MHz, chloroform-*d*) δ = 7.35 (s, 4H), 5.26−5.12 (m, 443H), 4.36 (q, 2H), 4.16−4.04 (m, 507H), 2.40−2.22 (m, 516H), 1.78−1.62 (m, 598H), 1.62−1.40 (m, 2137H), 0.97−0.86 (m, 770H).

Polymerization Kinetics. Polymerizations were assembled in 48 mL pressure vessels with a side arm adapter, under inert atmosphere in a glovebox. The vessel was taken out of the glovebox and the side arm was purged of air by cycling with vacuum and argon (×3). The pressure vessel was then placed in an oil bath at 130 °C. The start time for the polymerization was taken to be the time when the vessel was lowered into the oil bath. Aliquots were taken at various time points by placing the system under positive pressure of argon, opening the reaction vessel, taking an aliquot, closing the reaction vessel, and then closing the system to argon. The aliquots were quenched by cooling to 0 °C and samples for ^{1}H NMR spectroscopy and SEC analysis were prepared.

RESULTS

To afford γMCL (Figure S1 shows representative ^{1}H NMR spectra) in high conversion with limited side products, we employed a traditional Baeyer−Villiger oxidation using *meta*-chloroperoxybenzoic acid (*m*CPBA); alternatively, a green oxidant, oxone, can be used for this transformation.[18,19] After purification, the bulk polymerization of γMCL using a difunctional initiator, 1,4-benzenedimethanol (BDM), and the traditionally utilized ring-opening transesterification polymerization catalyst Sn(Oct)$_2$ afforded an α,ω-hydroxy telechelic polymer (Scheme 2, Figure S2). The bulk ring-opening

Scheme 2. Synthesis of PγMCL and LA-γMCL-LA

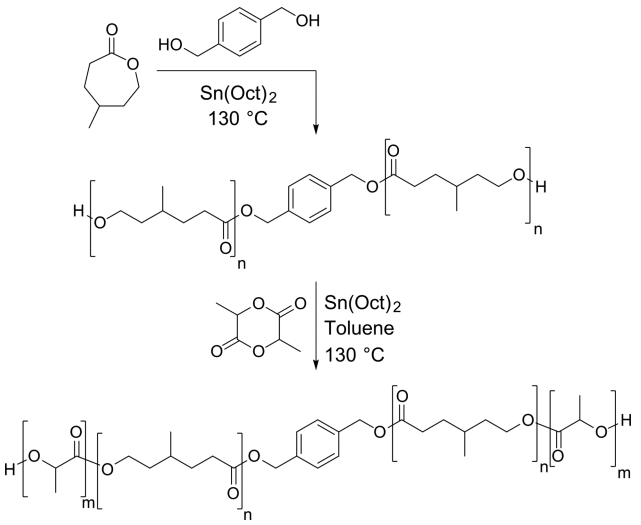

transesterification polymerization at 130 °C ([γMCL]$_0$ = 7.95 M, [BDM]$_0$ = 0.051 M, and [Sn(Oct)$_2$]$_0$ = 0.016 M) was monitored over time by taking aliquots of the polymerization for analysis by ^{1}H NMR spectroscopy and size exclusion chromatography (SEC). The reaction reached 95% conversion after 1 h and near quantitative conversion (∼99%) after 2 h (Figure 1a). Above 95% conversion, an increase in molar mass dispersity is evident due to intermolecular transesterification and/or equilibration phenomena, as described previously.[46,47] A linear relationship was observed between conversion and the molar mass of the polymer product (Figure 1b). The polymerization kinetics were first order in monomer, (Figure 1a, inset); however, the intercept appears to be positive, indicating the presence of polymer at t = 0 min. This is likely a result of the esterification reactions that occur at room temperature when the monomer, catalyst, and initiator are initially mixed;[48] the mixture of reagents at room temperature shows evidence of ring-opened γMCL and a shift in the benzylic protons by ^{1}H NMR spectroscopy (Figure S3). The pseudo first order rate constant averaged over three experiments at this concentration of Sn(Oct)$_2$ and at 130 °C is 0.050 min^{-1} (Figure S4). Assuming first order in catalyst concentration,[49] the average second order rate constant is 3.1 M^{-1} min^{-1}. The polymerization of γMCL catalyzed by Sn(Oct)$_2$ efficiently yields PγMCL with controlled molar mass and low dispersity.

The polymerization of *rac*-lactide (known as D,L-(±)-lactide or LA) or (*S*,*S*)-lactide (known as L-(−)-lactide or LLA) from telechelic PγMCL catalyzed by Sn(Oct)$_2$ was carried out in toluene at 130 °C (Scheme 2). The SEC traces show the growth of the polymer with no evidence of lower molar mass shoulders (representative data is shown Figure 2) and ^{1}H NMR spectroscopy shows a chemical shift of the end group (Figure S5). Analysis of the PγMCL homopolymer via ^{13}C NMR spectroscopy indicates a distinct singlet in the carbonyl region

DOI: 10.1021/acs.biomac.7b00283
Biomacromolecules 2017, 18, 1845−1854

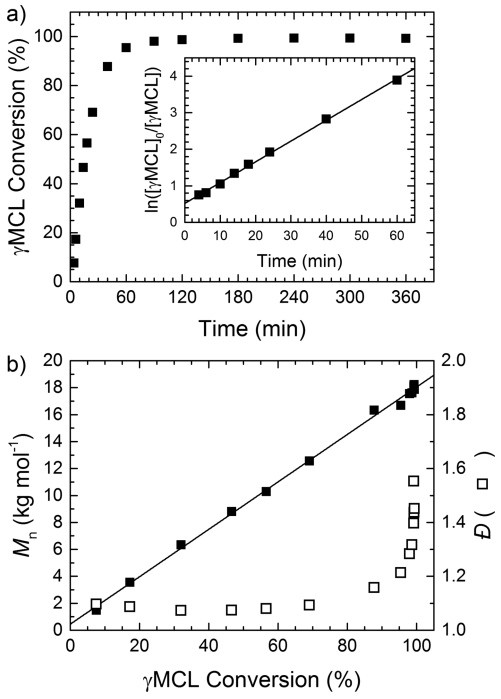

Figure 1. Bulk polymerization of γMCL at 130 °C, $[\gamma MCL]_0$ = 7.96 M, $[BDM]_0$ = 0.051 M, $[Sn(Oct)_2]_0$ = 0.016 M. (a) Conversion of γMCL determined by ^{1}H NMR spectroscopy as a function of time. The inset shows a linear fit of the kinetic data up to 60 min, where the reaction reaches 95% conversion. (b) Molar mass (■) determined by end group analysis shows a linear relationship with conversion.

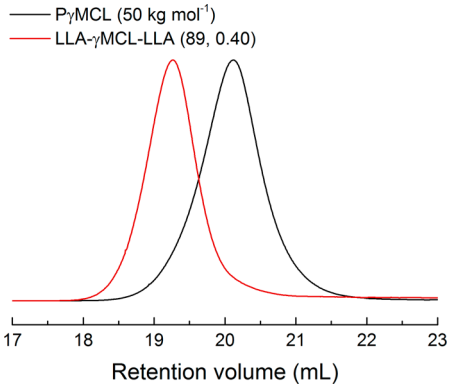

Figure 2. Overlay of chloroform SEC traces for triblock polymer from 50 kg mol^{-1} PγMCL.

that corresponds to a γMCL repeat unit adjacent to two γMCL units. In triblock copolymers, this PγMCL resonance remains unchanged with a second feature visible for PLA and PLLA in LA-γMCL-LA and LLA-γMCL-LLA samples, respectively (Figure S6).[50] The appearance of two features that correspond to the respective homopolymers indicates that highly pure blocks were formed with no evidence of transesterification between blocks.[18,19] A set of low molar mass volumetrically symmetric polymers with various molar masses were synthesized to determine the temperature-dependent interaction parameter $\chi(T)$ while high molar mass polymers with various volume fractions of PLA were synthesized to study the mechanical properties for TPE applications. PLA-TPEs with PγMCL as the midblock were easily synthesized utilizing traditional polymerization catalyst and elevated temperature, providing control over molar mass and composition with low dispersity.

In a set of relatively low molar mass triblock samples, two glass transitions were observed by differential scanning calorimetry (DSC): one for the PγMCL block (−58 to −55 °C) and one for the PLA blocks (35 to 45 °C; Table 1, Figure S7). The observed glass transition temperature for PLA is lower than that of the high molar mass homopolymer, likely due to the low molar mass of the PLA blocks. Small-angle X-ray scattering (SAXS) patterns of low molar mass polymers show long-range order, and the samples with equivalent volume fractions of each block show reflections for lamellar morphology (Figure S8). Room temperature SAXS patterns and the evidence of two glass-transition temperatures corroborate the triblock polymers are microphase separated.

Triblock polymers of low molar mass and equivalent volume fractions of PLA and PγMCL were melt-pressed at 70−110 °C to obtain uniform disks for dynamic mechanical thermal analysis (DMTA) experiments. A sample was placed between two 25 mm diameter parallel plates and the storage modulus was monitored while heating at 1 °C min^{-1} and oscillating at 1 rad s^{-1}. The order−disorder transition temperature T_{ODT} is evident by the precipitous drop in modulus (Figure 3, right, and Figure S9). Dynamic frequency sweeps below and above the ODT demonstrate that this drop in modulus is a result of the ODT (Figures S10 and S11). We report results from both LA-γMCL-LA (20A, 0.49) and LA-γMCL-LA (20B, 0.49), though the samples appear to be identical, as they exhibit a different T_{ODT} due to the slight difference in molar mass. A triblock polymer LA-γMCL-LA (27, 0.51) was also analyzed with temperature controlled SAXS, heating through the order−disorder transition, corroborating the results observed using DMTA (Figure 3, left, and Figure S12). Plotting χ as a function of T^{-1} obtained from DMTA experiments, the temperature dependent interaction parameter $\chi(T)$ given in eq 1 was determined (Figure S9) using $(\chi N)_{ODT}$ = 17.996 and a

Table 1. Summary of Symmetric (f_{LA} ~ 0.5) Block Polymers

sample ID ($M_{n,total}$, f_{LA})	$M_{n,P\gamma MCL}$ [a] (kg mol^{-1})	$M_{n,PLA}$ [a] (kg/mol)	$M_{n,total}$ [a] (kg/mol)	f_{LA} [b]	$Đ$ [c]	$T_{g,P\gamma MCL}$ [d] (°C)	$T_{g,PLA}$ [d] (°C)	T_{ODT} [e] (°C)
LA-γMCL-LA (20A, 0.49)	9.2	11	20	0.49	1.15	−55	36	84
LA-γMCL-LA (20B, 0.49)	9.3	11	20	0.49	1.14	−57	37	92
LA-γMCL-LA (23, 0.49)	10	12	23	0.49	1.17	−56	40	113
LA-γMCL-LA (27, 0.49)	12	14	27	0.49	1.25	−56	44	138
LA-γMCL-LA (27, 0.51)	12	15	27	0.51	1.16	−58	37	140
LA-γMCL-LA (30, 0.51)	13	17	30	0.51	1.20	−57	45	165

[a]Determined using end-group analysis of ^{1}H NMR. [b]Calculated using ρ_{PLA} = 1.25 g cm^{-3} and $\rho_{P\gamma MCL}$ = 1.037 g cm^{-3} at 25 °C. [c]Chloroform SEC analysis with PS standards. [d]Determined as the midpoint of the inflection on second heating at 10 °C min^{-1} in a DSC. [e]Determined from the precipitous drop in DMTA heating at 1 °C min^{-1}.

DOI: 10.1021/acs.biomac.7b00283
Biomacromolecules 2017, 18, 1845−1854

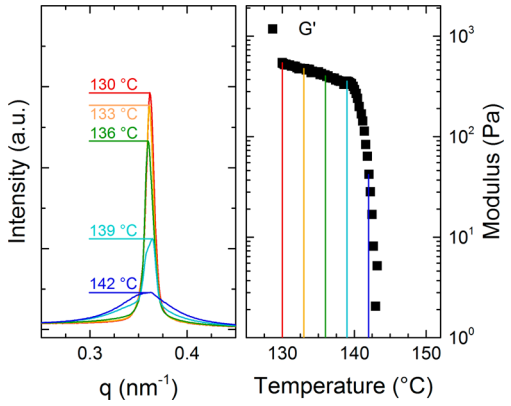

Figure 3. SAXS analysis (left) and DMTA (right) upon heating showing ODT for LA-γMCL-LA (27, 0.51). For SAXS analysis, a sample was heated to the designated temperature, annealed 2 min, and then analyzed. The decrease in the sharpness and intensity of the principle peak indicate the ODT at approximately 140 °C. The same polymer was subjected to DMTA where the ODT is indicated by the precipitous drop, also around 140 °C, in modulus upon heating at 1 °C min^{-1} in 25 mm plates with ω = 1 rad s^{-1} and 1% strain.

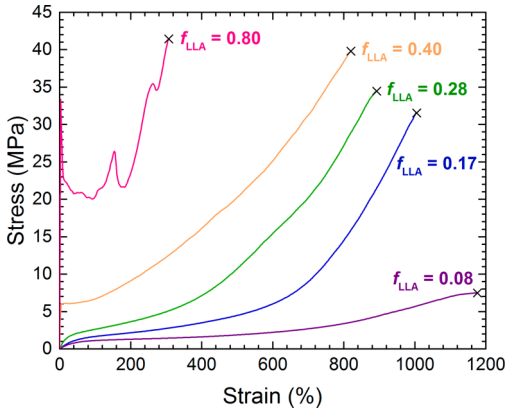

Figure 4. Representative stress−strain curves of thermoplastic elastomers with varying fractions of PLLA, extended at 50 mm min^{-1}, with the break point indicated by ×.

reference volume of 118 Å^3 to calculate the degree of polymerization N.[51]

$$\chi(T) = \frac{51.6 \pm 2.1}{T} - (0.07 \pm 0.01) \quad (1)$$

The ODTs for the samples in Table 1 were observed above the T_g of PLA and below the temperature where 5% mass is lost in the sample ($T_{d,5\%} \sim 260$ °C, Figure S13).

To demonstrate the versatile properties of these new triblock polymers with PLLA end blocks and PγMCL midblock, the mechanical properties were determined for polymers with volume fractions of PLLA 0.08 to 0.80 (Table 2). The polymers were melt-pressed at 180 °C, quenched, and cut into dog bone shapes yielding transparent and colorless samples. These bars were left to age for 1 day at RT then a minimum of 5 samples were tested under uniaxial extension at a rate of 50 mm min^{-1} until break. A representative set of data for each sample pulled to its breaking point is shown in Figure 4 and averaged results with the standard deviation are summarized in Table 2. The sample with the lowest composition of PLLA (f_{LLA} = 0.08) does not exhibit the strain-hardening behavior observed in the other samples, resulting in a low ultimate tensile strength due to the short PLA chains. Samples with f_{LLA} of 0.17 and 0.28 exhibit low Young's modulus values and high elongations at break, typical of elastomeric behavior. These samples strain-harden, resulting in impressive average ultimate tensile strengths of 31 and 35 MPa, respectively. Cyclical extension of LLA-γMCL-LLA (159, 0.17) to 1000% strain and subsequent relaxation to 0% strain indicates that the strain-hardening behavior is irreversible; much less stress is required to deform this sample after the first cycle (Figure S14). Samples with a higher PLLA content (f_{LLA} = 0.80) exhibit high yield points and then plastic deformation. DSC analysis of tensile bars before and after testing show an increase in enthalpy of fusion upon the first heat corroborating strain-induced crystallization in the hard blocks (Figure S15). The jagged features seen in the stress−strain curve of LLA-γMCL-LLA (159, 0.80) were present through all five samples that were tested (Figure S16), likely a result of the irregularities apparent in the bars from processing. Based on this sample set, the strain at break decreases as the mass fraction of PLLA increases (Figure S17). These samples with semicrystalline PLA, LLA-γMCL-LLA, exhibit excellent tensile properties, with high tensile strengths and elongations at break.

Table 2. Summary of High Molar Mass Triblock Polymers with Mechanical Properties

sample ID ($M_{n,total}$, f_{LA})	$M_{n,P\gamma MCL}$[a] (kg/mol)	$M_{n,PLA}$[a] (kg/mol)	$M_{n,total}$[a] (kg/mol)	f_{LA}[b]	$Đ$[c]	$T_{g,P\gamma MCL}$[d] (°C)	$T_{g,PLA}$[d] (°C)	T_m[e] (°C)	E[f] (MPa)	σ_B[f] (MPa)	ε_B[f] (%)
LLA-γMCL-LLA (150, 0.08)	135	15	150	0.08	1.31	−60		159	2.2 ± 0.1	7.8 ± 0.5	1190 ± 60
LLA-γMCL-LLA (159, 0.17)	127	32	159	0.17	1.36	−59	47	162	4.0 ± 0.3	31 ± 4	1200 ± 30
LLA-γMCL-LLA (73, 0.28)	50	23	73	0.28	1.11	−59	52	163	13 ± 10	35 ± 3	895 ± 20
LLA-γMCL-LLA (89, 0.40)	50	40	89	0.40	1.07	−60	54	169	18 ± 10	37 ± 6	786 ± 90
LLA-γMCL-LLA (159, 0.80)	27	132	159	0.80	1.26	−65	56	175	1300 ± 30	42 ± 3	314 ± 20
LA-γMCL-LA (94, 0.17)	76	18	94	0.17	1.34	−60	42		4.8 ± 0.2	24 ± 2	1029 ± 20
LLA-γMCL-LLA (95, 0.17)	76	19	95	0.17	1.32	−59	47	162	3.6 ± 0.1	30 ± 4	988 ± 30

[a]Determined using end-group analysis of ^{1}H NMR. [b]Calculated using ρ_{PLA} = 1.25 g cm^{-3} and $\rho_{P\gamma MCL}$= 1.037 g cm^{-3} at 25 °C. [c]Chloroform SEC analysis with PS standards. [d]Determined as the midpoint of the inflection on second heat at 10 °C min^{-1} in a DSC. [e]Determined as the peak temperature on second heat at 10 °C min^{-1} in a DSC. [f]Determined from tensile testing to the break point of 5 samples extended at 50 mm min^{-1}.

DOI: 10.1021/acs.biomac.7b00283
Biomacromolecules 2017, 18, 1845−1854

To study the effect of crystallinity in PLA on the mechanical properties of TPEs, block polymers of the same molar mass with a small volume fraction of PLA were synthesized. Polymerizing LA or LLA from 76 kg mol^{-1} PγMCL, a complementary pair of block polymers with atactic end blocks (LA-γMCL-LA) and isotactic end blocks (LLA-γMCL-LLA) were obtained with f_{LA} = 0.17 (Table 2). SAXS patterns of LA-γMCL-LA and LLA-γMCL-LLA with f_{LA} = 0.17 exhibit a principle scattering peak with broad secondary peaks (Figure S4). The morphology assignment is not definitive due to the lack of long-range order, though the broad secondary peaks resemble spherical form-factor scattering.[52] Both block polymers exhibited glass transitions for PγMCL and PLA, and LLA-γMCL-LLA exhibited an additional melting transition by DSC at 162 °C with 21% crystallinity during the second heat.

Films of LA-γMCL-LA and LLA-γMCL-LLA with f_{LA} = 0.17 were subjected to extensional DMTA experiments, monitoring the modulus as a function of temperature (Figure 5). The glass

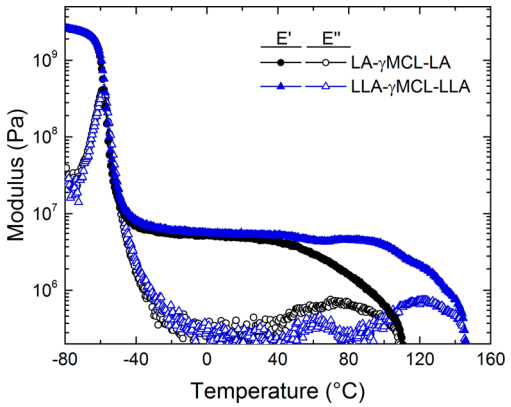

Figure 5. Extensional DMTA of triblock polymers comparing the storage modulus (solid) and loss modulus (open) of (black) LA-γMCL-LA (94, 0.17) and (blue) LLA-γMCL-LLA (95, 0.17) heating at 5 °C min^{-1}.

transition, taken as the peak of tan δ, occurs at −59 °C for the PγMCL block and corroborates the glass transition temperature of PγMCL obtained from DSC (Table 2, Figure S18). The modulus of the rubbery plateau region allows evaluation of the level of entanglements in the rubbery PγMCL midblock. Using the Guth-Smallwood approximation with the assumption that the PLA domains are spherical hard domains acting as a filler in PγMCL rubber, the entanglement molar mass was calculated M_e = 2.8 kg mol^{-1}, which agrees with the entanglement molar mass M_e = 2.9 kg mol^{-1} obtained from the linear viscoelastic behavior of 92 kg mol^{-1} PγMCL (Figures S19−21).[53] The rubbery plateau for both samples occurs at the same modulus, indicating that changing the crystalline nature of PLLA does not influence the stiffness of these TPEs. However, changing the end block affects the softening temperature indicated by a decrease in modulus; LA-γMCL-LA begins to soften at the T_g of 45 °C while LLA-γMCL-LLA exhibits solid-like behavior up to 100 °C.

LA-γMCL-LA exhibits high ultimate tensile strength of 24 MPa and LLA-γMCL-LLA exhibits an even higher strength (Figure 6, Table 3), consistent with similar studies.[13,16] The higher tensile strength in LLA-γMCL-LLA is a result of strain-induced crystallization in PLLA, which enhances the strain-hardening behavior. These two elastomeric samples were subjected to cyclic loading of 300% strain at 50 mm min^{-1}

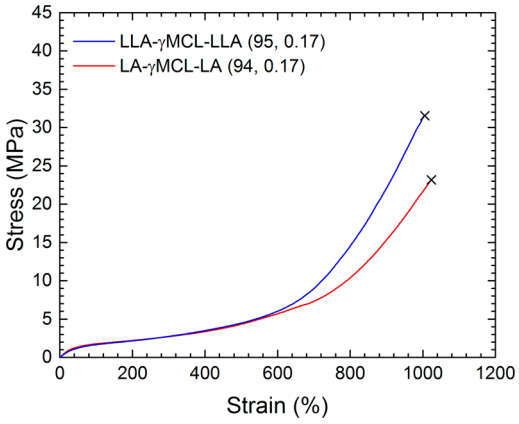

Figure 6. Comparison of block polymers of PLA and PLLA with similar molar mass and composition. Representative stress−strain curves from five melt-pressed dog bones pulled at 50 mm min^{-1} to its break point ×.

for 10 cycles to explore their hysteresis behavior (Figure 7). There is some energy loss in the first cycle for LA-γMCL-LA and the stress at 300% continues to decrease in subsequent cycles. In contrast, LLA-γMCL-LLA exhibits much lower energy loss with a small decrease in stress at 300% in subsequent cycles. As the residual strain observed is dependent on the initial level of strain imposed, thus, the ratio of residual strain to the subjected strain is reported. Hysteresis experiments were run in triplicate, providing a range of residual strains for LA-γMCL-LA of 0.12−0.17 and LLA-γMCL-LLA of 0.06−0.07. In summary, the semicrystalline PLA end blocks impart higher temperature resistance and are more resilient than the samples with amorphous PLA end blocks.

To further study the difference in permanent deformation observed in hysteresis experiments, LA-γMCL-LA and LLA-γMCL-LLA with f_{LA} = 0.17 were subjected to stress-relaxation experiments. A step-strain of 25% was imparted on the samples at various temperatures, and the modulus was monitored over 3 h (Figure 8). Samples studied at 0 °C for LLA-γMCL-LLA and −40 °C for LA-γMCL-LA show a small decrease in modulus with time. This is likely from the relaxation of the stressed amorphous PγMCL block that is above its T_g. At temperatures of 40 °C and above, both TPEs show a decrease in the normalized modulus to various amounts beyond the relaxation from PγMCL, where LA-γMCL-LA relaxes at a much faster rate than LLA-γMCL-LLA. Interestingly, LA-γMCL-LA exhibits significant stress relaxation at room temperature (T = 20 °C). The higher permanent deformation exhibited by amorphous PLA-TPEs when subjected to a step-strain corroborates the increased energy loss shown in hysteresis testing for the same samples.

DISCUSSION

The polymerizability of lactones has been a significant research topic as the size of the lactone, position of substituent, and size of substituent affect the thermodynamics and kinetics of polymerization.[30] A recent in-depth study demonstrated that the size of the lactone largely affects the thermodynamics of polymerization, while the position and nature of the substituent largely affects the kinetics of polymerization.[26] The thermodynamic favorability to form polyesters from ε-caprolactones provides a synthetic advantage over δ-valerolactones. Of methyl-substituted ε-caprolactones that yield low-T_g polyesters,

DOI: 10.1021/acs.biomac.7b00283
Biomacromolecules 2017, 18, 1845−1854

Table 3. Summary of the Mechanical Properties of PLA-TPEs with Reports of the Entanglement Molar Mass and the Segment−Segment Interaction Parameter

PLA-TPE	$M_{n,total}$ (kg mol^{-1})	f_{LA}	E (MPa)	σ_B (MPa)	ε_B (%)	$M_{e,rubbery}$ (kg mol^{-1})	χ (140 °C)	ref
LLA-γMCL-LLA	73	0.28	13 ± 10	35 ± 3	895 ± 20	2.9	0.055	this work
LLA-βMVL-LLA	107.2	0.32	5.9 ± 0.9	28 ± 4	1720 ± 140	4.3	0.036	13, 26
LLA-M-LLA	41.8	0.34	1.5 ± 0.1	13.6 ± 1.4	900 ± 76	11−14	NR	16
LA-γMCL-LA	94	0.17	4.8 ± 0.2	24 ± 2	1030 ± 20	2.9	0.055	this work
LA-εMCL-LA	122	0.16	1.9 ± 0.1	10.2 ± 0.8	1880 ± 70	3.0	0.048	19, 21
LA-CD-LA	104	0.17	1.5 ± 0.3	9.9 ± 0.6	2100 ± 100	3.9	0.041	21
LA-βMVL-LA	103.6	0.29	1.9 ± 0.6	9.0 ± 1.1	1790 ± 130	4.3	0.036	13, 26
LA-D-LA	136	0.21	1.0 ± 0.1	4.5 ± 0.3	1600 ± 200	5.9	0.095	20, 21

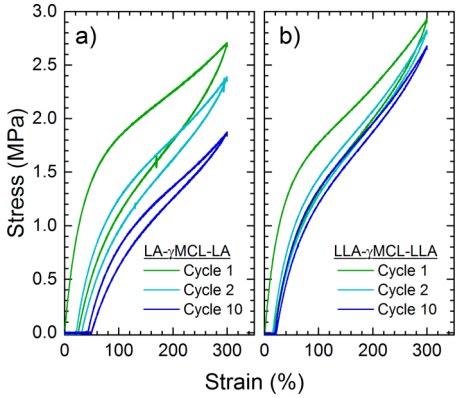

Figure 7. Hysteresis of (a) LA-γMCL-LA (94, 0.17) and (b) LLA-γMCL-LLA (95, 0.17) of 10 cycles of 300% strain at 50 mm min^{-1}.

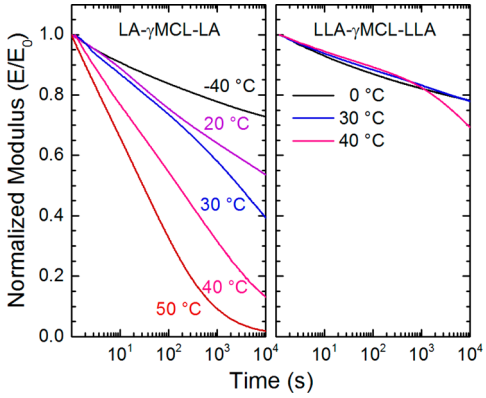

Figure 8. Stress relaxation of LA-γMCL-LA (94, 0.17) and LLA-γMCL-LLA (95, 0.17). Samples were subjected to an instantaneous 25% strain at various temperatures and the modulus was monitored for 3 h.

the kinetics of γMCL polymerization are significantly faster (95% conversion after 1 h) compared to εMCL (95% conversion after more than 3 h) under the same catalyst loading and reaction conditions.[19] The change in propagating group from secondary to primary alcohol and a less sterically hindered ester results in a significant increase in the rate of polymerization for γMCL.

The range of aliphatic polyester PLA-TPEs reported in literature provide us the opportunity to explore the key parameters that affect the mechanical properties in the resultant TPEs. However, because of the different sample preparation conditions and testing parameters used, quantitative comparisons can be challenging. Changing the ratio between blocks controls the morphology of the bulk material impacting the mechanical properties; an increase in PLLA content results in an increase in ultimate tensile strength and Young's modulus and a decrease in elongation at break (Figure 4).[54] PγMCL incorporated as the minority component LLA-γMCL-LLA (159, 0.80) showed high modulus and high elongation at break for a majority PLLA sample, demonstrating PγMCL acts as a toughening filler in PLLA when incorporated into a block polymer architecture. This result agrees with other reports that utilize block polymers, where the identity of the midblock impacts the toughness of the overall block polymer.[29] When block polymers demonstrate a spherical morphology, with glassy A blocks and rubbery B blocks, samples exhibit elastomeric behavior. A high performance PLA-TPE previously reported, LLA-βMVL-LLA (107, 0.32), exhibited σ_B = 28 ± 4 MPa and ε_B = 1720 ± 140%.[13] We report a sample with a similar composition and lower overall molar mass, LLA-γMCL-LLA (72.9, 0.28), that exhibits a higher average ultimate tensile strength σ_B = 35 ± 3 MPa albeit with lower elongation at break ε_B = 895 ± 20%. This increase in ultimate tensile strength and decrease in elongation at break has been observed in PS-TPEs, where SBS has higher strength and lower elongation in comparison to SIS.[4] This result has long been attributed to the differences in the midblock entanglement molar mass: $M_{e,PI}$ = 5.0 kg mol^{-1} and $M_{e,PB}$ = 1.6 kg mol^{-1}.[4] The same trend is seen in these PLA-TPEs, where a decrease in entanglement molar mass provides high strength TPEs (Table 3). These data support the hypotheses that a lower entanglement molar mass leads to more trapped entanglements per volume in the rubbery midblock, which adds strength to the material.

An increase in the segment−segment interaction parameter between blocks has also been shown to improve ultimate tensile strength and decrease elongation at break.[4] To further highlight this effect, a polymerization method that results in styrene repeat units in the rubbery midblock results in an imperfect block polymer that has a lower χ between blocks and leads to a decrease in material strength.[55] Ring-opening transesterification polymerization facilitates control over molar mass; however, side transesterification reactions can result in randomization of the chain and increased dispersity. Though these side reactions can be beneficial for the synthesis of random copolymers, such as poly(ε-caprolactone-*co*-LLA), it also means that when targeting an A-B-A architecture, the A and B blocks can randomize, effectively reducing χ. The ^{13}C NMR spectra of polyester TPEs provide evidence for distinct blocks for TPEs reported in Table 3. When changing the midblock from PβMVL to PγMCL, there is an increase in χ, as well as a decrease in the entanglement molar mass, which contribute to the increase in tensile strength and decrease in elongation at break (Table 3).

DOI: 10.1021/acs.biomac.7b00283
Biomacromolecules 2017, 18, 1845−1854

LA-γMCL-LA demonstrates more than double the stress at break, albeit with a lower elongation at break compared to LA-εMCL-LA.[19] PγMCL and PεMCL have very similar entanglement molar masses, $M_{e,P\gamma MCL}$ = 2.9 kg mol^{-1} and $M_{e,P\varepsilon MCL}$ = 3.0 kg mol^{-1}; thus, the degree of entanglements does not explain this impact in the mechanical properties.[21] Although the chemical nature of these polymers only differs by the change in the position of the methyl substituent, their segment−segment interaction parameter χ with PLA is slightly different (Table 3). As Martello et al. point out, the values reported for the tensile properties of LA-εMCL-LA are likely lower limits. Further studies to resolve these discrepancies are underway.

With a PγMCL midblock and f_{LA} = 0.17, the use of isotactic PLLA over atactic PLA improved the ultimate tensile stress by 7 MPa, while maintaining an elongation at break of ∼1000% (Table 2). Previous studies that directly compare the mechanical properties between PLA-TPEs with atactic PLA and isotactic PLLA also support this trend: PLLA end block TPEs exhibit significantly higher ultimate tensile strength while maintaining identical elongations at break.[13,16,56] TPEs have two types of physical cross-links: trapped entanglements in the rubbery domain and microphase-separated glassy/semicrystalline domains. To avoid complications from crystallization breakout disrupting the microphase-separated morphology, samples were quenched during processing. The trapped entanglements are dynamic and dictate the extensibility of the rubbery midblock, limiting the elongation at break for comparative samples.[6] Using the same rubbery midblock, the maximum tensile strength for a TPE system depends heavily on the nature of the hard end block, all other parameters being equal (molar mass, composition, and χ).

Impressively, LLA-γMCL-LLA exhibited half the residual strain when compared to the PLA counterpart, indicating PLLA-TPEs have lower permanent deformation after extension (Figure 7). The largest energy loss occurs in the first cycle of extension, common for this class of compounds, which can be attributed to the alignment of the hard domains in the direction of extension or deformation of the domains themselves.[57,58] Subsequent cycles show stress softening, also known as the Mullins effect.[59] When extending LLA-γMCL-LLA to extreme elongations, 1000% strain, the strain-hardening behavior from strain-induced crystallization exhibited in the stress−strain curve is not reversible upon relaxation, only through reprocessing, though prestraining the material does result in the ability to strain the material to the same elongation with less stress.

Stress relaxation studies indicate that the atactic PLA end blocks are soft enough at 20 °C to allow the TPEs to relax upon an applied stress (Figure 7). Similar studies on microphase-separated SIS TPEs show a crossover temperature, where the behavior transitions from permanent to transient cross-links at 30 °C, significantly below the T_g of PS.[60] Above 30 °C, SIS TPEs under extension experience relaxation as a result of chain-pullout, wherein the PS chain slips out of the glassy domain, which reduces the stress exhibited by the sample. The PLA chains in LA-γMCL-LA are likely experiencing similar chain-pullout near room temperature. The extent of chain-pullout increases closer to the glass transition temperature of PLA that consequently increases the rate at which stress is diminished. The temperature-dependent χ also decreases as the system is heated. These more complex behaviors close to the T_g of PLA resulted in the failure of time−temperature superposition (TTS) for stress relaxation results.[61] This chain-pullout theory at moderate temperatures provides an explanation for the increased permanent deformation and lower ultimate tensile strengths observed in amorphous PLA-TPEs. In contrast, PLLA-TPEs show relaxation after long times (hours) when the temperature is near the glass transition temperature of the PLLA blocks. We hypothesize that elastomers with PLLA exhibit lower permanent deformation due to the crystallinity in the hard domains that help prevent chain-pullout. Crystallinity is not the only method to reduce chain-pullout of the hard A block, as it can also be mitigated by utilizing star or multiblock architectures.[62,63]

CONCLUSION

We report the efficient and practical synthesis of an aliphatic polyester TPE system LA-γMCL-LA with precise control over molar mass with low dispersity. The high density of trapped entanglements in the rubbery midblock, dictated by the low entanglement molar mass of PγMCL, controls the extensibility of the TPE. The LA-γMCL-LA elastomers exhibit excellent mechanical properties, including the highest ultimate tensile strength reported to date for this class of materials. This is a result of the combination of high molar mass polymers, low entanglement molar mass of the rubbery block, and moderate incompatibility between the rubbery and glassy blocks. The permanent deformation seen in amorphous PLA-TPEs is likely a result of chain-pullout upon an applied stress and can be mitigated using semicrystalline PLA as the end block. Semicrystalline end blocks allow for a wider operating temperature window and even better mechanical performance; the ultimate tensile strength is higher and there is very little permanent deformation when compared to the amorphous PLA-TPE counterpart. This study demonstrates the key parameters that contribute to the mechanical strength seen in ABA block polymer TPEs and corroborates the behaviors observed in PS-TPEs. The properties observed in LA-γMCL-LA TPEs expand our understanding for the design of high performance sustainable TPEs.

ASSOCIATED CONTENT

Supporting Information

The Supporting Information is available free of charge on the ACS Publications website at DOI: 10.1021/acs.biomac.7b00283.

Additional figures (S1−S21) and information on DMTA experiments (PDF).

AUTHOR INFORMATION

Corresponding Author

*E-mail: hillmyer@umn.edu.

ORCID

Annabelle Watts: 0000-0003-2310-3961

Marc A. Hillmyer: 0000-0001-8255-3853

Present Address

†Department of Mechanical Engineering, Keio University, Yokohama 223−8522, Japan.

Funding

This work was funded by the Center for Sustainable Polymers, a NSF-supported Center for Chemical Innovation (CHE-1413862), at the University of Minnesota.

DOI: 10.1021/acs.biomac.7b00283
Biomacromolecules 2017, 18, 1845−1854

Notes

The authors declare the following competing financial interest(s): The authors declare the competing financial interest of Marc A. Hillmyer who is on the Board of Directors, serves as secretary, and has equity and royalty interests in Valerian materials, a company commercializing MVL and of The University of Minnesota who has equity and royalty interests in Valerian Materials. These interests have been reviewed and managed by the University of Minnesota in accordance with its Conflict of Interest policies. The other authors declare no competing financial interest.

■ ACKNOWLEDGMENTS

We would like to acknowledge Jacob Brutman for consultation on extensional DMTA experiments, as well as Guilhem De Hoe, Stacey Saba, Sam Dalsin, Deborah Schneiderman, and James Gallagher for many helpful discussions. We thank Ortec, Inc. for their generous donation of lactide. SAXS experiments were performed at the DuPont-Northwestern-Dow Collaborative Access Team (DND-CAT) located at Sector 5 of the Advanced Photon Source (APS). DND-CAT is supported by Northwestern University, E.I. DuPont de Nemours & Co., and The Dow Chemical Company. This research used resources of the Advanced Photon Source, a U.S. Department of Energy (DOE) Office of Science User Facility operated for the DOE Office of Science by Argonne National Laboratory under Contract No. DE-AC02-06CH11357. Data was collected using an instrument funded by the National Science Foundation under Award Number 0960140.

■ REFERENCES

(1) World Economic Forum, Ellen MacArthur Foundation, and McKinsey and Company. The New Plastics Economy: Rethinking the Future of Plastics, 2016; http://www.ellenmacarthurfoundation.org/publications.

(2) Anastas, P.; Eghbali, N. Green Chemistry: Principles and Practice. *Chem. Soc. Rev.* **2010**, *39*, 301−312.

(3) Dubé, M. A.; Salehpour, S. Applying the Principles of Green Chemistry to Polymer Production Technology. *Macromol. React. Eng.* **2014**, *8*, 7−28.

(4) *Thermoplastic Elastomers*, 3rd ed.; Holden, G., Kricheldorf, H. R., Quirk, R. P., Eds.; Hanser Gardner Publications, Inc.: Cincinnati, 2004.

(5) Holden, G.; Bishop, E. T.; Legge, N. R. Thermoplastic Elastomers. *J. Polym. Sci., Part C: Polym. Symp.* **1969**, *26*, 37−57.

(6) Tong, J.; Jerôme, R. Dependence of the Ultimate Tensile Strength of Thermoplastic Elastomers of the Triblock Type on the Molecular Weight between Chain Entanglements of the Central Block. *Macromolecules* **2000**, *33*, 1479−1481.

(7) Shin, J.; Kim, Y.-W.; Kim, G.-J. Sustainable Block Copolymer-Based Thermoplastic Elastomers. *Kongop Hwahak* **2014**, *25*, 121−133.

(8) Hillmyer, M. A.; Tolman, W. B. Aliphatic Polyester Block Polymers: Renewable, Degradable, and Sustainable. *Acc. Chem. Res.* **2014**, *47*, 2390−2396.

(9) Pitt, C. G.; Gratzl, M. M.; Kimmel, G. L.; Surles, J.; Schindler, A. Aliphatic Polyesters II. The Degradation of Poly (D,L-lactide), Poly (ε-caprolactone), and Their Copolymers in Vivo. *Biomaterials* **1981**, *2*, 215−220.

(10) Loefgren, A.; Albertsson, A.-C.; Dubois, P.; Jerome, R.; Teyssie, P. Synthesis and Characterization of Biodegradable Homopolymers and Block Copolymers Based on 1,5-Dioxepan-2-One. *Macromolecules* **1994**, *27*, 5556−5562.

(11) Albertsson, A.-C.; Varma, I. K. Recent Developments in Ring Opening Polymerization of Lactones for Biomedical Applications. *Biomacromolecules* **2003**, *4*, 1466−1486.

(12) Cohn, D.; Hotovely Salomon, A. Designing Biodegradable Multiblock PCL/PLA Thermoplastic Elastomers. *Biomaterials* **2005**, *26*, 2297−2305.

(13) Xiong, M.; Schneiderman, D. K.; Bates, F. S.; Hillmyer, M. a.; Zhang, K. Scalable Production of Mechanically Tunable Block Polymers from Sugar. *Proc. Natl. Acad. Sci. U. S. A.* **2014**, *111*, 8357−8362.

(14) Huang, Y.; Chang, R.; Han, L.; Shan, G.; Bao, Y.; Pan, P. ABA-Type Thermoplastic Elastomers Composed of Poly(ε-Caprolactone-co-δ-Valerolactone) Soft Midblock and Polymorphic Poly(Lactic Acid) Hard End Blocks. *ACS Sustainable Chem. Eng.* **2016**, *4*, 121−128.

(15) Ryner, M.; Albertsson, A.-C. Resorbable and Highly Elastic Block Copolymers from 1,5-Dioxepan-2-One and L-Lactide with Controlled Tensile Properties and Hydrophilicity. *Biomacromolecules* **2002**, *3*, 601−608.

(16) Wanamaker, C. L.; Bluemle, M. J.; Pitet, L. M.; O'Leary, L. E.; Tolman, W. B.; Hillmyer, M. A. Consequences of Polylactide Stereochemistry on the Properties of Polylactide-Polymenthide-Polylactide Thermoplastic Elastomers. *Biomacromolecules* **2009**, *10*, 2904−2911.

(17) Wanamaker, C. L.; O'Leary, L. E.; Lynd, N. A.; Hillmyer, M. A.; Tolman, W. B. Renewable-Resource Thermoplastic Elastomers Based on Polylactide and Polymenthide. *Biomacromolecules* **2007**, *8*, 3634−3640.

(18) Shin, J.; Martello, M. T.; Shrestha, M.; Wissinger, J. E.; Tolman, W. B.; Hillmyer, M. A. Pressure-Sensitive Adhesives from Renewable Triblock Copolymers. *Macromolecules* **2011**, *44*, 87−94.

(19) Martello, M. T.; Hillmyer, M. A. Polylactide-Poly(6-Methyl-ε-Caprolactone)-Polylactide Thermoplastic Elastomers. *Macromolecules* **2011**, *44*, 8537−8545.

(20) Martello, M. T.; Schneiderman, D. K.; Hillmyer, M. A. Synthesis and Melt Processing of Sustainable Poly(ε-Decalactone)-Block-Poly(Lactide) Multiblock Thermoplastic Elastomers. *ACS Sustainable Chem. Eng.* **2014**, *2*, 2519−2526.

(21) Schneiderman, D. K.; Hill, E. M.; Martello, M. T.; Hillmyer, M. A. Poly(Lactide)-Block-Poly(ε-Caprolactone-co-ε-Decalactone)-Block-Poly(Lactide) Copolymer Elastomers. *Polym. Chem.* **2015**, *6*, 3641−3651.

(22) Cohn, D.; Hotovely Salomon, A. Designing Biodegradable Multiblock PCL/PLA Thermoplastic Elastomers. *Biomaterials* **2005**, *26*, 2297−2305.

(23) Kong, J. F.; Lipik, V.; Abadie, M. J. M.; Roshan Deen, G.; Venkatraman, S. S. Characterization and Degradation of Elastomeric Four-Armed Star Copolymers Based on Caprolactone and L-Lactide. *J. Biomed. Mater. Res., Part A* **2012**, *100A*, 3436−3445.

(24) Kong, J. F.; Lipik, V.; Abadie, M. J.; Deen, G. R.; Venkatraman, S. S. Biodegradable Elastomers Based on ABA Triblocks: Influence of End-Block Crystallinity on Elastomeric Character. *Polym. Int.* **2012**, *61*, 43−50.

(25) Nakayama, Y.; Aihara, K.; Yamanishi, H.; Fukuoka, H.; Tanaka, R.; Cai, Z.; Shiono, T. Synthesis of Biodegradable Thermoplastic Elastomers from ε-Caprolactone and Lactide. *J. Polym. Sci., Part A: Polym. Chem.* **2015**, *53*, 489−495.

(26) Schneiderman, D. K.; Hillmyer, M. A. Aliphatic Polyester Block Polymer Design. *Macromolecules* **2016**, *49*, 2419−2428.

(27) Brutman, J. P.; De Hoe, G. X.; Schneiderman, D. K.; Le, T. N.; Hillmyer, M. A. Renewable, Degradable, and Chemically Recyclable Cross-Linked Elastomers. *Ind. Eng. Chem. Res.* **2016**, *55*, 11097−11106.

(28) Martello, M. T.; Burns, A.; Hillmyer, M. Bulk Ring-Opening Transesterification Polymerization of the Renewable δ-Decalactone Using an Organocatalyst. *ACS Macro Lett.* **2012**, *1*, 131−135.

(29) Olsén, P.; Borke, T.; Odelius, K.; Albertsson, A.-C. ε-Decalactone: A Thermoresilient and Toughening Comonomer to poly(L-Lactide). *Biomacromolecules* **2013**, *14*, 2883−2890.

(30) Olsén, P.; Odelius, K.; Albertsson, A.-C. Thermodynamic Presynthetic Considerations for Ring-Opening Polymerization. *Biomacromolecules* **2016**, *17*, 699−709.

DOI: 10.1021/acs.biomac.7b00283
Biomacromolecules 2017, 18, 1845−1854

(31) Breteler, M. R. T.; Zhong, Z.; Dijkstra, P. J.; Palmans, A. R. A.; Peeters, J.; Feijen, J. Ring-Opening Polymerization of Substituted ε-Caprolactones with a Chiral (Salen) AlOiPr Complex. *J. Polym. Sci., Part A: Polym. Chem.* **2007**, *45*, 429−436.
(32) Peeters, J. W.; van Leeuwen, O.; Palmans, A. R. A.; Meijer, E. W. Lipase-Catalyzed Ring-Opening Polymerizations of 4-Substituted ε-Caprolactones: Mechanistic Considerations. *Macromolecules* **2005**, *38*, 5587−5592.
(33) Seefried, C. G.; Koleske, J. V. Lactone Polymers. VI. Glass-Transition Temperatures of Methyl-Substituted ε-Caprolactones and Polymer Blends. *J. Polym. Sci., Polym. Phys. Ed.* **1975**, *13*, 851−856.
(34) Xiao, Y.; Cummins, D.; Palmans, A. R. A.; Koning, C. E.; Heise, A. Synthesis of Biodegradable Chiral Polyesters by Asymmetric Enzymatic Polymerization and Their Formulation into Microspheres. *Soft Matter* **2008**, *4*, 593−599.
(35) Zupancich, J. A.; Bates, F. S.; Hillmyer, M. A. Aqueous Dispersions of Poly(Ethylene Oxide)-b-Poly(γ-Methyl-ε-Caprolactone) Block Copolymers. *Macromolecules* **2006**, *39*, 4286−4288.
(36) Chen, M.; Zhang, Y.; Zhou, Y.; Zhang, Y.; Lang, M.; Ye, Z.; Tan, W. S. Pendant Small Functional Groups on Poly(ε-Caprolactone) Substrate Modulate Adhesion, Proliferation and Differentiation of Human Mesenchymal Stem Cells. *Colloids Surf., B* **2015**, *134*, 322−331.
(37) Lee, R.; Huang, Y.; Chen, W. Synthesis and Characterization of Temperature-Sensitive Block Copolymers from Poly(N-isopropylacrylamide) and 4-Methyl-ε-Caprolactone or 4-Phenyl-ε-Caprolactone. *J. Appl. Polym. Sci.* **2010**, *118*, 1634−1642.
(38) Lee, R.-S.; Hung, C.-B.; Huang, Y.; Chen, W. Synthesis and Characterization of Amphiphilic Block Copolymers from Poly(Ethylene Glycol)Methyl Ether and 4-Methyl-ε-Caprolactone or 4-Phenyl-ε-Caprolactone. *Polymer* **2007**, *48*, 2605−2612.
(39) Rainbolt, E. A.; Washington, K. E.; Biewer, M. C.; Stefan, M. C. Recent Developments in Micellar Drug Carriers Featuring Substituted Poly(ε-Caprolactone)s. *Polym. Chem.* **2015**, *6*, 2369−2381.
(40) Vangeyte, P.; Jérôme, R. Amphiphilic Block Copolymers of High-Molecular-Weight Poly(Ethylene Oxide) and Either ε-Caprolactone or γ-Methyl-ε-Caprolactone: Synthesis and Characterization. *J. Polym. Sci., Part A: Polym. Chem.* **2004**, *42*, 1132−1142.
(41) Fiege, H. Cresols and Xylenols. *Ullmann's Encyclopedia of Industrial Chemistry*; Wiley-VCH Verlag GmbH & Co. KGaA: Weinheim, Germany, 2000; pp 419−461.
(42) Roberge, D. M.; Buhl, D.; Niederer, J. P. M.; Hölderich, W. F. Catalytic Aspects in the Transformation of Pinenes to p-Cymene. *Appl. Catal., A* **2001**, *215*, 111−124.
(43) Linnekoski, J. A.; Asikainen, M.; Heikkinen, H.; Kaila, R. K.; Räsänen, J.; Laitinen, A.; Harlin, A. Production of p-Cymene from Crude Sulphate Turpentine with Commercial Zeolite Catalyst Using a Continuous Fixed Bed Reactor. *Org. Process Res. Dev.* **2014**, *18*, 1468−1475.
(44) Schutyser, W.; Van Den Bosch, S.; Dijkmans, J.; Turner, S.; Meledina, M.; Van Tendeloo, G.; Debecker, D. P.; Sels, B. F. Selective Nickel-Catalyzed Conversion of Model and Lignin-Derived Phenolic Compounds to Cyclohexanone-Based Polymer Building Blocks. *ChemSusChem* **2015**, *8*, 1805−1818.
(45) Panthani, T. R.; Bates, F. S. Crystallization and Mechanical Properties of Poly(L-Lactide)-Based Rubbery/Semicrystalline Multiblock Copolymers. *Macromolecules* **2015**, *48*, 4529−4540.
(46) Albertsson, A.-C.; Varma, I. K. Recent Developments in Ring Opening Polymerization of Lactones for Biomedical Applications. *Biomacromolecules* **2003**, *4*, 1466−1486.
(47) Martello, M. T.; Burns, A.; Hillmyer, M. Bulk Ring-Opening Transesterification Polymerization of the Renewable δ-Decalactone Using an Organocatalyst. *ACS Macro Lett.* **2012**, *1*, 131−135.
(48) Kricheldorf, H. R.; Kreiser-Saunders, I.; Stricker, A. Polylactones 48. $SnOct_2$-Initiated Polymerizations of Lactide: A Mechanistic Study. *Macromolecules* **2000**, *33*, 702−709.
(49) Witzke, D. R.; Narayan, R.; Kolstad, J. J. Reversible Kinetics and Thermodynamics of the Homopolymerization of L-Lactide with 2-Ethylhexanoic Acid Tin(II) Salt. *Macromolecules* **1997**, *30*, 7075−7085.
(50) In't Veld, P. J. A.; Velner, E. M.; Van De Witte, P.; Hamhuis, J.; Dijkstra, P. J.; Feijen, J. Melt Block Copolymerization of ε-Caprolactone and L-Lactide. *J. Polym. Sci., Part A: Polym. Chem.* **1997**, *35*, 219−226.
(51) Wu, L.; Cochran, E. W.; Lodge, T. P.; Bates, F. S. Consequences of Block Number on the Order-Disorder Transition and Viscoelastic Properties of Linear $(AB)_N$ Multiblock Copolymers. *Macromolecules* **2004**, *37*, 3360−3368.
(52) Frick, E. M.; Zalusky, A. S.; Hillmyer, M. A. Characterization of Polylactide-b-Polyisoprene-b-Polylactide Thermoplastic Elastomers. *Biomacromolecules* **2003**, *4*, 216−223.
(53) Guth, E. Theory of Filler Reinforcement. *J. Appl. Phys.* **1945**, *16*, 20−25.
(54) Honeker, C. C.; Thomas, E. L. Impact of Morphological Orientation in Determining Mechanical Properties in Triblock Copolymer Systems. *Chem. Mater.* **1996**, *8*, 1702−1714.
(55) Cunningham, R. E.; Auerbach, M.; Floyd, W. J. Preparation and Stress−strain Properties of SBS and SIS Block Polymers Made with Dilithium Initiators. *J. Appl. Polym. Sci.* **1972**, *16*, 163−173.
(56) Zhang, Z.; Grijpma, D. W.; Feijen, J. Triblock Copolymers Based on 1,3-Trimethylene Carbonate and Lactide as Biodegradable Thermoplastic Elastomers. *Macromol. Chem. Phys.* **2004**, *205*, 867−875.
(57) Zhao, Y.; Ning, N.; Hu, X.; Li, Y.; Chen, F.; Fu, Q. Processing Temperature Dependent Mechanical Response of a Thermoplastic Elastomer with Low Hard Segment. *Polymer* **2012**, *53*, 4310−4317.
(58) Tomita, S.; Lei, L.; Urushihara, Y.; Kuwamoto, S.; Matsushita, T.; Sakamoto, N.; Sasaki, S.; Sakurai, S. Strain-Induced Deformation of Glassy Spherical Microdomains in Elastomeric Triblock Copolymer Films: Simultaneous Measurements of a Stress−Strain Curve with 2d-SAXS Patterns. *Macromolecules* **2017**, *50*, 677−686.
(59) Payne, A. R. Hysteresis in Rubber Vulcanizates. *J. Polym. Sci., Polym. Symp.* **1974**, *48*, 169−196.
(60) Hotta, A.; Clarke, S. M.; Terentjev, E. M. Stress Relaxation in Transient Networks of Symmetric Triblock Styrene-Isoprene-Styrene Copolymer. *Macromolecules* **2002**, *35*, 271−277.
(61) Han, C. D.; Baek, D. M.; Kim, J. K.; Ogawa, T.; Sakamoto, N.; Hashimoto, T. Effect of Volume Fraction on the Order-Disorder Transition in Low Molecular Weight Polystyrene-Block-Polyisoprene Copolymers. 1. Order-Disorder Transition Temperature Determined by Rheological Measurements. *Macromolecules* **1995**, *28*, 5043−5062.
(62) Burns, A. B.; Register, R. A. Mechanical Properties of Star Block Polymer Thermoplastic Elastomers with Glassy and Crystalline End Blocks. *Macromolecules* **2016**, *49*, 9521−9530.
(63) Matsumiya, Y.; Watanabe, H.; Takano, A.; Takahashi, Y. Uniaxial Extensional Behavior of $(SIS)_P$-Type Multiblock Copolymer Systems: Structural Origin of High Extensibility. *Macromolecules* **2013**, *46*, 2681−2695.

DOI: 10.1021/acs.biomac.7b00283
Biomacromolecules 2017, 18, 1845−1854